AVALANCHE PROBABILITY: SLAB RELEASE AND THE EFFECT OF FOREST COVER

Peter Gauer[1,*]

[1]*Norwegian Geotechnical Institute, Norway*

ABSTRACT: One of the main challenges in regard to hazard mapping is to estimate avalanche probabilities and avalanche size for a given path. One reason for this is the lack of sufficient data. By definition, avalanches of interest for hazard mapping (typically avalanches of relative size R4 or R5) are rare events and in addition, their detailed observations are often hindered by bad weather and hazardous conditions. Another question is How influences forest cover the avalanche hazard. It is commonly accepted that dense forests is the most cost effective mitigation against natural avalanche release. However, little work has been done to quantify of the effect of forest cover on the release probability of avalanches. In this paper, we present a Monte-Carlo simulation approach, first, to obtain estimates on avalanche release probabilities and probability distributions of the expected fracture depth—which is an important parameter for modern numerical avalanche models—depending on climatological parameters. Then we extend the model to account for the supporting effect of forest on the snowpack. In this way, it becomes possible to quantify the efficiency of a forest and to define requirements on a forest stand as a protective forest.

Preliminary results of the model show that the obtained tendencies are consistent with observations and are in the expected range.

Keywords: avalanche probability, avalanche size, hazard mapping, forest

1. INTRODUCTION

In many mountain areas with seasonal or year round snow cover, snow avalanches endanger the population and its infrastructure, like houses and communications lines.

It is widely accepted that hazard mapping is one of the most cost effective protection measures. Avalanche hazard maps highlight areas endangered. Typically, danger zones are delimited according to a nominal annual exceedance probability P_a of a specified avalanche intensity. The corresponding nominal return period $T_r = 1/P_a$.

Avalanche hazard is influenced by combination of various parameters, like:

- terrain (slope, exposition, roughness, ...);
- vegetation (stand density, tree diameter, undergrow, ...) ;
- precipitation (frequency, amount, intensity, rain, snow, ...);
- wind
- snowpack properties (maritime, continental, ...)
- runout distance

One can imagine that avalanche hazard is determined by a series of conditional probabilities, which are difficult to define. To be able to obtain despite of this complication a quantification on the hazard it is common to distinguish between release probability and probable run-out distance. In this case, avalanche hazard H may be given by

$$H = P_R \, P_S \,, \tag{1}$$

where P_R is the avalanche release probability and P_S is that probability that the avalanche actually reaches a specified point along the track. The latter is influenced of the mobility of the avalanche. In (1), both probabilities are regarded as independent (e.g. Schläppy et al., 2014), which is a hardly justifiable assumption. Furthermore, for simplicity, the avalanche release probability is typically linked to the three-day new snow HNW_{3d} (McClung and Schaerer, 2006; Salm et al., 1990). That this approach might be overly conservative was indicated by Schweizer et al. (2008). In addition, HNW_{3d} has also been directly linked to the fracture depth (c.f. Salm et al., 1990), which is an important parameter for most of the modern avalanche models. Linking the fracture depth just with HNW_{3d} may, however, cause in many cases an underestimation of initial release mass.

The influence of forest on the avalanche hazard is a long lasting question. It is commonly accepted that dense forests is the most cost effective mitigation against natural avalanche release (Olschewski et al., 2012; Bebi et al., 2001). The protection is on the one hand due to the changed snowpack properties within the forest showing less frequent extended weak-layers (Gubler and Rychetnik, 1991; Teich et al., 2016). On the other hand, tree trunks have a supporting effect on the snowpack. Less estab-

*Corresponding author address:
Peter Gauer, Norwegian Geotechnical Institute,
P.O. Box 3930 Ullevl Stadion, NO–0806 Oslo, Norway
Tel: ++47 45 27 47 43; Fax: ++47 22 23 04 48; E-mail: pg@ngi.no

lished are criteria that define which stand structure is sufficient to prevent avalanche releases (Meyer-Grass and Schneebeli, 1992; Ishikawa et al., 1969; Viglietti et al., 2010) or that describe the braking efficiency of the forest for flowing avalanches (Feistl et al., 2014).

The aim of this paper is to present a model that can be used as tool to estimate return periods and corresponding release properties suitable as input parameter for avalanche runout models. The model is simple enough to be executed in a Monte-Carlo simulation approach, but still reflects the most important physical aspects of avalanche release, and it can be run on readily available input data to account for varying climatic conditions. By extending the initial model, the protective effect of a forest stand can considered. This will allow for its quantification.

2. MODEL

2.1. Simple Model

The fracture of an slab avalanche is a multistage process. An overview on the latest stage of knowledge can be found in Schweizer et al. (2016). For the purpose to define an avalanche release probability with respect to natural release and hazard mapping, we restrict ourself to a simple model that allow for a probabilistic approach. To this end, we extend the simple model of Lackinger (1989) for our aim. However, the model distinguishes two probabilities, 1) probability of failure of the weak-layer and 2) the probability that the slab actually overcomes the residual friction between bed-surface and slab and starts to slide. The latter is treated as independent of the first one.

For nomenclature see Fig. 1 and Fig. 2. In the first step, we consider the performance function

$$G = R - L\,, \tag{2}$$

where R is the resistance and L the load. The case of an avalanche release is marked by $G < 0$. For an initial stable snow pack,

$$G_0 = R_0 - L_0 > 0\,, \tag{3}$$

where the driving load L_0 from the snowpack is

$$L_0 = \rho_{sb}\, g\, \sin\phi\, H_{sb} \cos\phi\,. \tag{4}$$

The initial resistance R_0 is given by the combination of the strength of the weak-layer, τ_{wl}, and the support due to the tensional and shear strength along the crown, stauchwall, and flanks of the slab. R_0 may be approximated as

$$R_0 = \tau_{WL} + \frac{D_{sb}}{L_{sb}} \left(\sigma_{sb} + \tau_{sb} \left(\sqrt{2} + 2\, r_{LB}\right)\right)\,, \tag{5}$$

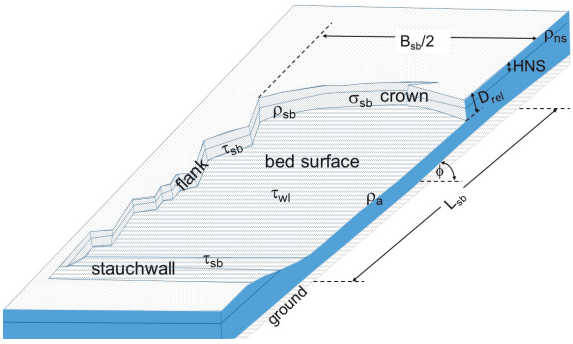

Figure 1: Slab avalanche nomenclature.

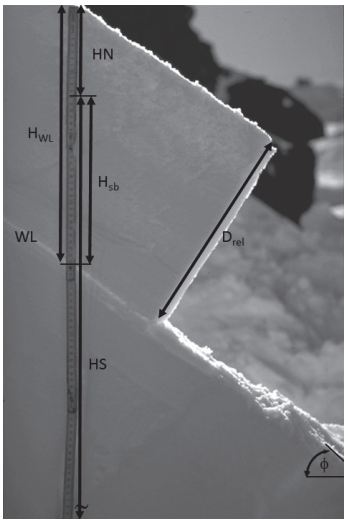

Figure 2: Sketch of a snow slab; HN is the new snow depth, HS the (old) snow depth, H_{WL} the depth of the weak-layer *WL* below the surface, $H_{sb} = H_{WL} - HN$ the height of the slab and ϕ is the slope angle (photo by courtesy of J. Schweizer).

where σ_{sb} and τ_{sb} are the tensional strength and shear strength of the slab, L_{sb} is the slab length and the ratio $r_{LB} = L_{sb}/B_{sb}$, and B_{sb} is the slab width. r_{LB} is supposedly of order of 1 (e.g. McClung, 2009). The slab thickness of the slab $D_{sb} = H_{sb} \cos\phi$. Figures 1 and 2 illustrate some of the used geometric parameters. As can be seen from (5), the support due to the slab itself rapidly diminishes with increasing slab size, and the resistance is dominated by the shear strength of the weak-layer.

Natural avalanche release occurs, if the initially stable snowpack is overloaded or its resistance is decreased. Here we focus on the first case where overloading can occur due to an increase of new snow or snow drift. In the model, the modified performance function is

$$G = (R_0 + \Delta R) - (L_0 + \Delta L)\,, \tag{6}$$

where the increase in loading is

$$\Delta L = g\, \sin\phi\, \mathrm{HNW} \cos\phi\,. \tag{7}$$

Here, HNW is the snow water equivalent of the additional snow load either due to new snow or snow

drift. In the model, HNW = HNW_{3d} + HNW_{drift}. The change of the resistance term is modeled as

$$\Delta R = I_{Fac}\left(\Delta_{t\tau}\tau_{WL} + \frac{D_{ns}}{L_{sb}}\left(\sigma_{ns} + \tau_{ns}\left(\sqrt{2} + r_{LB}\right)\right)\right). \quad (8)$$

D_{ns} (= $\mathrm{HNW}\cos\phi/\rho_{ns}$) is the thickness of the new snow layer and ρ_{ns} is its density. I_{Fac} accounts for the intensity of loading and decreases with increasing loading intensity. The increase of the weak-layer strength during loading is modeled by a cohesive term and an additional Coulomb-friction like contribution. The ansatz in Eqs. (8) is inspired of measurements in Zeidler (2004) and in Jamieson et al. (2007).

The probability, P_{lS}, that the slab detached, fragments, and starts to slide may be approximated by the probability to overcome the residual friction

$$P_{lS} = 1 - P(\mu_{cf} > \tan\phi), \quad (9)$$

where μ_{cf} is the crack-face friction factor (c.f. van Herwijnen and Heierli, 2009; Simenhois et al., 2012).

2.2. Extended Model

In the extended model, the mechanical support by a forest is accounted by including an additional resistance term, that is,

$$G_0 = (R_0 + R_{f0}) - L_0 \quad (10)$$

and

$$G = (R_0 + R_{f0} + \Delta R + \Delta R_f) - (L_0 + \Delta L). \quad (11)$$

Following the approach according to the Swiss guidelines (Margreth, 2007; Ancey and Bain, 2015) for the force of the snowpack on a mast like obstacle—and vice versa—, the mechanical support of a forest stand might be approximated by

$$R_{f0} = F1\, K(s,\phi)\left(\rho_s \mathrm{HS}^2 - \rho_{sb}(\mathrm{HS} - H_{sb})^2\right), \quad (12)$$

where

$$F_1 = \frac{1}{2}\,\mathrm{dN}\,\eta_f\, N_g\, g\cos\phi. \quad (13)$$

The stand factor dN (in unit m^{-1}) is defined by $N_{ha}\,d/10^4$, where N_{ha} is the number of trees per hectare projected area and d is the diameter of the trees. $\eta_f = 1 + c\,\mathrm{HS}\cos(\phi)/d$, and where c is an empirical gliding factor that ranges from 0.6 (low gliding rate) to 6 (high gliding rate); typically, $c \approx 1.5$. As the critical stem diameter for breakage and the maximum snow depth is correlated η_f might be approximated as $\eta_f \approx 1 + 0.15\cos(\phi)$, avoiding the explicit need of knowing the stem diameter. Haefeli's creep factor K can be given as

$$K(s,\phi) = \sin(2\phi)(2.5\,s^3 - 1.86\,s^2 + 1.06\,s + 0.54), \quad (14)$$

with $s = \rho/\rho_w$ and ρ_w is the density of water. K ranges typically between 0.5 and 0.9. Haefelis's glide N_g varies from between 1.2 (rough slopes) and 3.2 (smooth slopes) (cf. Margreth, 2007). The additional forest support due to the new snow is approximated by

$$\Delta R_f = F_1\, K(s_m,\phi)\,\rho_m\,(\mathrm{HS} + \mathrm{HN})^2 - R_{f0}. \quad (15)$$

where HN = HNW/ρ_{ns}, $\rho_m = (\rho_s\mathrm{HS} + \rho_{ns}\mathrm{HN})/(H_{sb} + \mathrm{HN})$, and $s_m = \rho_m/\rho_w$.

2.3. Conditional probability $P(A|HNW_{3d})$

The conditional probability $P(A|\mathrm{HNW}_{3d})$ of observing an avalanche for given HNW_{3d} involves climatic as well terrain information and is therefore an important factor to describe avalanche probability for a given location. It can be obtained from Eqs. (2) and (3) by evaluating the ratio of observed failures to initially stable realisations for varying snowpack and loading conditions. For this purpose, a Monte-Carlo simulation approach is used, where only days with snow on the ground are considered to determine input distributions for HS, SWE, HNW_{3d}, and T_a (to be more efficient).

2.4. Avalanche frequency

The avalanche frequency can be estimated by the integral of the conditional probability of slide release assuming an additional loading due to precipitation times the daily probability that the amount of precipitation occurs over all possible accumulations, that is

$$P_{f1d} = \int_0^\infty P(A|\mathrm{HNW}_{3d})\,P(\mathrm{HNW}_{3d})\,d\mathrm{HNW}_{3d}. \quad (16)$$

Then, this probability is combined with the probability that the slab actually start sliding

$$P_{R1d} = P_{f1d}\,P_{lS}. \quad (17)$$

The combination provides an expected daily avalanche probability. To obtain an annual avalanche frequency this needs yet to be adjusted by the number of days in a year with snow on the ground (i.e. actually allowing for avalanches).

3. Parameter estimates

For the Monte-Carlo simulation, distribution functions for the various parameters are needed that reflect the climatic conditions at the location of interest.

3.1. Climatic input data

The model requires probability distributions for HS, SWE, HNW_{1d} or HNW_{3d}, and T_a. For Norway, we used the time series of winter data from SeNorge (Saloranta, 2014), which provides data on a 1 km grid for snow height HS_{ex}, snow water equivalent SWE_{ex}, HNW_{1dex} snow water equivalent for new snow and the air temperature T_{aex}. This time series are bilinear interpolated from neighboring grid cells to the point of interest and than fitted to parameter distributions from which can be chosen at random. HNW_{1dex} is also used to obtain the three day new snow water equivalent HNW_{3dex}. Here, we use the subscript $\bullet_{ex}$ to mark that these parameters refer to the measured times series (external data) instead of random variables used for the Monte-Carlo simulation.

3.2. Density approximations

The density is one of the most important characteristics of a snowpack and it reflects in a large degree winter weather conditions and climatic conditions. To derive a suitable distribution functions for the average density ρ_s of the whole snowpack depending on HS, which can be used in the Monte-Carlo simulation, the following relation is used

$$\rho_s = c_{r2}\mathrm{HS}^{c_{r3}} + c_{r1} + \Delta_{rnd\rho_s} \,. \tag{18}$$

The parameters c_{r1}, c_{r2}, and c_{r3} are obtained by parameter fitting of SWE_{ex}/HS_{ex} to HS_{ex}. In this way, we account for the conditions at the location of interest. $\Delta_{rnd\rho_s}$ is an appropriate random part also reflecting the observations.

For ρ_{ns}, we follow the approach implemented in SeNorge

$$\rho_{ns} \approx \rho_{nsmin} + 0.1 \max(0, 1.8\mathrm{T}_a + 32)^2 \tag{19}$$

with $\mathrm{T}_a < 1.3\,^\circ C$. Using the similarity approximation of Ling (1985) for the snow density versus snow depth, one can obtain estimates for

$$\rho_{mx} \approx \frac{\rho_s - dc1\rho_{s0}}{1 - dc1} \,, \tag{20}$$

$$\rho_a \approx \rho_{s0} + (\rho_{mx} - \rho_{s0})(1 - exp(-4r_{wl})) \,, \tag{21}$$

$$\rho_{sb} \approx \rho_{mx} - \frac{\rho_{mx} - \rho_{s0}}{(4r_{wl})}(1 - exp(-4r_{wl})) \,, \tag{22}$$

where ρ_{s0} is the density at the surface ($\approx \rho_{ns}$), ρ_a is the density adjacent to the weak-layer and ρ_{sb} is the mean density of the slab. Here we use $r_{wl} = H_{sb}/\mathrm{HS}$ and $dc1 \approx 0.25$. As little is know about typical weak-layer depth an uniform distribution is assumed for the simulations at present.

3.3. Snowpack strength parameter

As mentioned before, density is one of the most important characteristics of a snowpack and its strength characteristics. A number empirical approaches relate the shear strength and the tension strength to the density (Jamieson and Johnston, 1990a,b; Perla et al., 1982; Sigrist, 2006). In the Monte-Carlo model, we use

$$\sigma_{sb} = 10^{\left(c_{s2}\log_{10}(\rho_{sb}) + c_{s1} + \Delta_{rnd\sigma_{sb}}\right)} \,, \tag{23}$$

$$\tau_{sb} = 10^{\left(c_{t2}\log_{10}(\rho_{sb})^{c_{t3}} + c_{t1} + \Delta_{rnd\tau_{sb}}\right)} \,, \tag{24}$$

for σ_{sb} and τ_{sb} to model the strength of the slab and similar expressions to model the new snow layer. Again, Δ_{rnd*} marks an appropriate random contribution. Similar approaches exists to related the weak-layer shear strength to the density of the adjacent snow layers (Jamieson and Johnston, 2001; Perla, 1977). We use the approach

$$\tau_{WL0} = 10^{\left(c_{w2}\log_{10}(\rho_a) + c_{w1} + \Delta_{rnd\tau_{WL0}}\right)} \,. \tag{25}$$

As Jamieson and Johnston (2001) indicates, the weak-layer strength may depend on the crystal type and therefore on the prevailing climatic conditions. Alternatively, the weak-layer may be parameterized using the load directly instead of the density as proposed by Zeidler and Jamieson (2006).

Fig. 3 shows data fits and examples of Monte-Carlo realisations for σ_{sb}, τ_{sb}, and τ_{WL0}.

The change of the weak-layer strength in Eq. (8) is modeled by

$$\Delta_{t\tau} = c_\tau + (c_\mu + \Delta_{rndc\mu})\, g\, \mathrm{HNW} \cos^2\phi \,. \tag{26}$$

3.4. Avalanche dimensions

Observations and measurements suggest that the dimension and slab properties are correlated (Brown et al., 1972; McClung, 2009; Jamieson and Johnston, 1990b, 1992). Here, we use the ansatz

$$B_{sb} = C_{B_{sb}} \left(\frac{\sigma_{sb}}{\rho_{sb}\sin\phi}\right)^2 \tag{27}$$

and

$$L_{sb} = r_{LB} B_{sb} \tag{28}$$

to relate slab dimensions to slab properties. $C_{B_{sb}}$ and r_{LB} are defined by appropriate probabilities density functions (PDF). For example, ratio r_{LB} may depend on the degree of confinement of the release

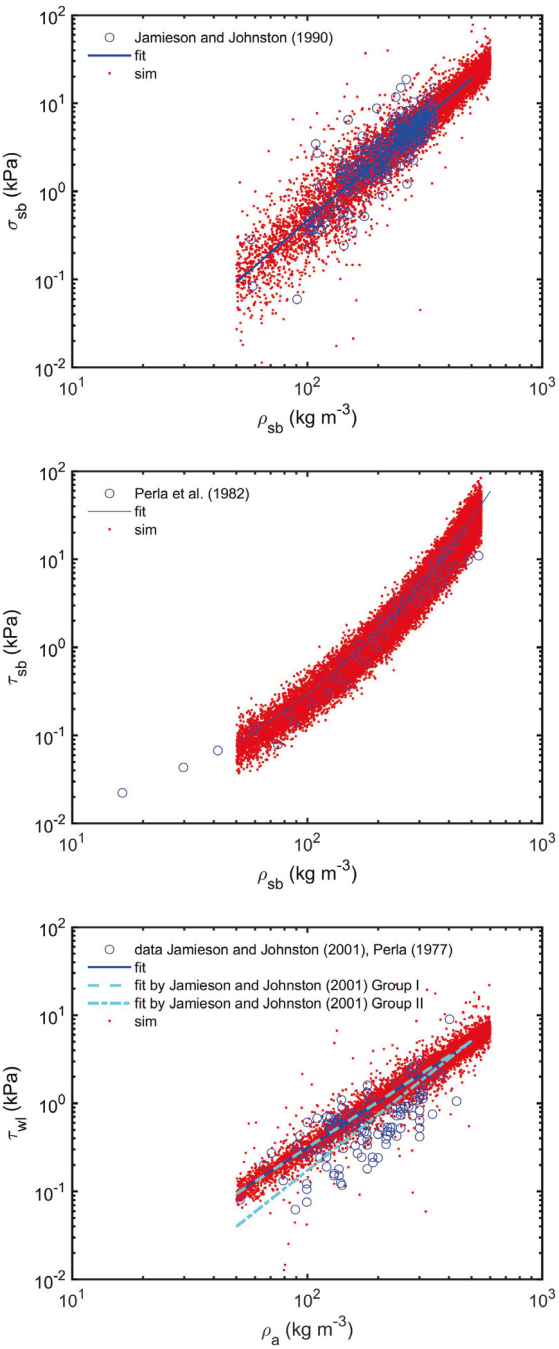

Figure 3: a) Tensional strength σ_{sb} and b) shear strength τ_{sb} vs slab density, ρ_{sb}; c) weak-layer shear strength, τ_{WL0} vs density of the adjacent layer, ρ_a. The figures show measurements from (Jamieson and Johnston, 1990a,b; Perla et al., 1982; Perla, 1977; Jamieson and Johnston, 2001) and references therein, data-fitting and examples of random realisation in the Monte-Carlo simulation.

area (e.g. McClung, 2009). r_{LB} is typically in the range of 0.2 to 5. The mean of $\overline{C}_{B_{sb}}$ is expected to be in the order of 0.2 (Jamieson and Johnston, 1990b).

3.5. Precipitation intensity

It is reasonable to assume that intense loading due to precipitation or snow drift gives the snowpack less time to adapt itself to the new stress conditions and causes an increase in natural avalanche releases. To account for this effect Eq. (8) involves an intensity factor which is define as

$$I_{Fac} = \exp(-i_{fc}\, I_{HN})\,, \tag{29}$$

where i_{fc} is an factor and

$$I_{HN} = g\, \max(\mathrm{HN3dt}, \mathrm{HN1dt}) \cos\phi \sin\phi\,. \tag{30}$$

Here, we use the three day intensity HN3dt = $(\mathrm{HNW}_{3d} + \mathrm{HNW}_{drift})/3$, where HNW_{drift} is a possible contribution due to snow drift, which can be positive or negative. Including HN1dt in Eq. (30), reflects the fact that the most recent intensity has a major effect on the release probability. To account for the correlation between three day intensity and one day intensity HN1dt, we use the relation HN1dt = HN3dt normrnd(1.3765, 0.44), which is based on observations from Gothic, Colorado.

3.6. Forest effect

Besides the direct support of the snowpack by tree trunks, forest influences also the snowpack proprieties and the intensity of loading due to interception. For example, the measurements by Teich et al. (2016) suggest a decrease of continues (weak-) layers with increase of crown cover. For the time being, in the Monte-Carlo model we account for this effect by linearly blending the weak-layer shear strength and the shear strength of the snowpack, that is

$$\tau_{WL} = (1 - f_{wgt})\tau_{WL0} + f_{wgt}\, \tau_{sb}\,, \tag{31}$$

where the weight factor is defined as $f_{wgt} = \min(1, \mathrm{dN}/\mathrm{dN}_0)$. The stand factor dN_0 will certainly depend on the tree species (conifer vs deciduous trees). To account for the second effect, the decrease in loading intensity, in the model, we reverse the time scale and decrease the time needed for the snowpack to adapt to the new loading conditions. That is, i_{fc} in Eq. (29) is modified by

$$i_{fc} = (1 - f_{wgt})i_{fc0} + f_{wgt}\, i_{fc1}\,. \tag{32}$$

c_τ and c_μ in Eq. (26) are adapted similarly.

4. MODEL RESULTS

In this section, we present preliminary model results and comparisons with measurements and observations to illustrate the general behavior.

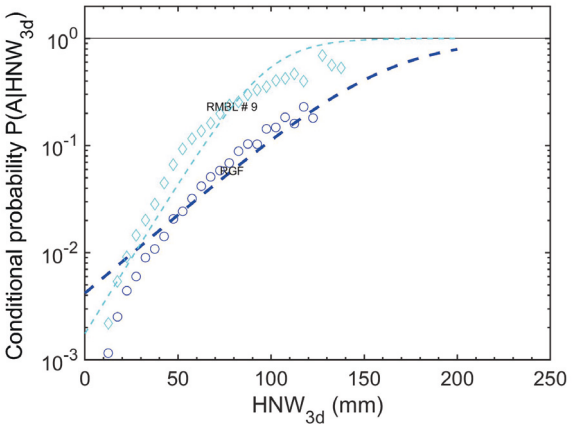

Figure 4: Distribution of the conditional probability $P(A|HNW_{3d})$. Comparison of observations (lines) and simulations (dots) for data from Gothic, Colorado (RMBL #9, $\phi \approx 37°$, τ_{WL}(Group II)) and Ryggfonn, Norway (RGF, $\phi \approx 43°$, τ_{WL}(Group I)).

Fig. 4 shows two simulations of the conditional probability $P(A|HNW_{3d})$, one for the climatic conditions corresponding to Ryggfonn, Norway, and the second one for conditions corresponding to Gothic, Colorado. For comparison, the figure includes results from logistic regression analysis of data from the Ryggfonn path and path #9 in Gothic. The model simulations reflect the general trend for both cases reasonably well. The by trend lower probability for Ryggfonn despite the steeper release area suggests an on average stronger snowpack. Considering the climatic conditions, that may be expected. That the model slightly underestimates the release probability for low precipitation events, especially for the Ryggfonn case, is inherent as the model does not include wet-snow events at present. Nonetheless, the model reproduces the avalanche frequency of about 2 to 4 per year in both cases.

Fig. 5 shows a comparison of the complementary cumulative distribution function (survival function) of D_{rel} for three simulations and data and proposed relations out of the literature (Rosenthal and Elder, 2003; McClung, 2003; Perla, 1977; Faillettaz et al., 2006; Gaume et al., 2012; Bazant et al., 2003). The simulation reflect the expected trend, however the direct comparison with the observation is difficult as those involve partially data collections from various path without speciation, e.g., of the slope angle or typical snow conditions. How the later may influence the expected release depth can be guessed from the comparison of the two simulation for Ryggfonn and Tromsdalen (both are run for same slope angle).

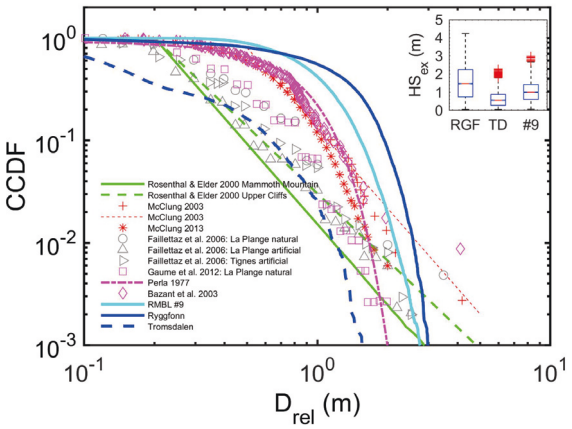

Figure 5: Complementary cumulative distribution function of D_{rel}. Comparison between simulations for Ryggfonn (Norway, $\phi \approx 43°$, τ_{WL}(Group I)), Tromsdalen (Norway, $\phi \approx 43°$, τ_{WL}(Group I)), and Gothic (Colorado, $\phi \approx 37°$, τ_{WL}(Group II)) and observations or proposed relations in the literature. The boxplot shows the snow height distributions for the three simulations.

The ratio between of D_{rel}/B_{sb} of the simulation for Rygfonn has a median of 95 and follows a lognormal distribution with $\mu_{BD} \approx 4.54$ and $\sigma_{BD} \approx 1.17$. For the simulation for Tromsdalen, the median is 263 ($\mu_{BD} \approx 5.57$; $\sigma_{BD} \approx 1.43$) and for RMBL #9, the median is 74 ($\mu_{BD} \approx 4.31$; $\sigma_{BD} \approx 1.24$). All three simulations are in agreement with published observations (c.f. McClung, 2009; Bair et al., 2010).

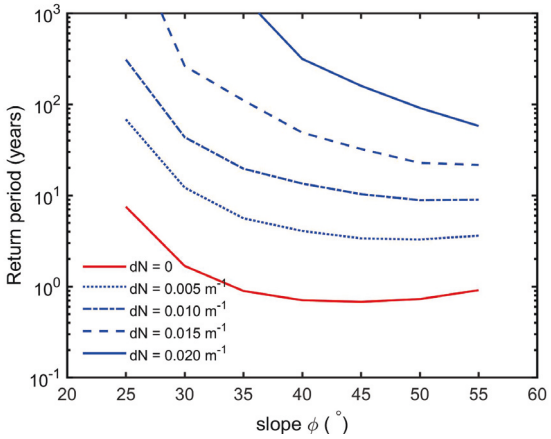

Figure 6: Comparison of the nominal return period vs mean slope angle of the release area with the stand factor dN as parameter (τ_{WL}(Group I)).

Fig. 6 now depicts a comparison of simulated return periods depending on slope angle and an assumed stand density dN for climatic data from Ryggfonn. The figure illustrates how the suggested protection effect of a forest increases with increasing stand factor dN and how increasing steepness of the release area reduces this increase. While the expected return period increases with increasing dN, the model implies that the expected water equivalent of the release, HW_{rel} (i.e. the release mass per projected area), decreases at the same time, as shown in Fig. 7. This decrease is accompanied by a change in avalanche characteristic from a more “old snow” dominated to “new snow” dominated failure. This new snow conditions on the other hand may favor higher mobility and relative long runouts.

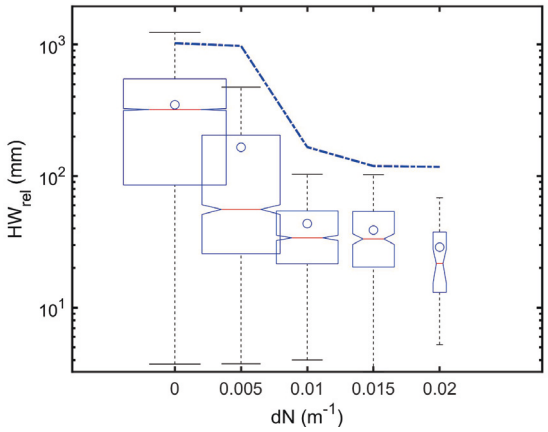

Figure 7: Comparison of the expected water equivalent of the release, HW_{rel}, vs stand factor dN. The (o) marks the mean value and width of the boxes indicates the relative number of expected releases. The dash-dotted line indicates the expected water equivalent of the release corresponding to a survival probability $S > 1/100$ (different from the return period; $\phi = 40°$; τ_{WL}(Group I))

5. CONCLUDING REMARKS

Avalanche risk management requires knowledge of avalanche release probability and expected runout, which both depend on the prevalent snow climate. The presented avalanche release model accounts for this.

Preliminary results of the model show that the obtained tendencies are consistent with observations and are in the expected order of magnitude. However, for a thorough verification of the model and to improve the parameterization more sets of suitable observations are required. Crucial is certainly the parameterization of the weak-layer shear strength and the intensity factor depending on the snow climate. The crack-friction has a major influence on if one finally observes an avalanche on moderately steep terrain or not. Little is also known about the typical distribution of the weak-layer depth.

It is widely accepted that a dense forest has a protective effect against avalanche release. However, there is no common consensus on the requirements on a forest stand as a protective forest. The model accounts for forest by including the support of the snowpack due to tree trunks and changing snowpack conditions. Again more and suitable observations are required to verify the approach.

Generally, trees in a forest can only support a cohesive snowpack. As soon as snowpack looses its bindings (e.g. due to very high water content) or the snowpack consist of low cohesive snow (e.g. Wildschneediamond snow or champagne powder) a forest loses its protective effect. In rare cases, avalanches have released in and have run through mature forests under such conditions (e.g. Hess, 1931). Not only these observations make it questionable to reliable quantify the protective effect of a forest in a perspective of a “1000-” or “5000-year” return period as it is required in the Norwegian regulations (TEK17, 2017).

ACKNOWLEDGMENTS

Parts of this research was financially supported by the Norwegian Ministry of Oil and Energy through the project grant R&D Snow avalanches 2017–2019 to NGI. The grant administrated by the Norwegian Water Resources and Energy Directorate (NVE). I thank billy barr for providing his avalanche observations from Gothic, Colorado.

REFERENCES

Ancey, C. and Bain, V. (2015). Dynamics of glide avalanches and snow gliding. *Reviews of Geophysics*, 53:745–784.

Bair, E. H., Birkeland, K. W., and Dozier, J. (2010). In situ and photographic measurements of avalanche crown transects. *Cold Regions Science and Technology*, 64:174–181.

Bazant, Z. P., Zi, G., and McClung, D. (2003). Size effect law and fracture mechanics of the triggering of dry snow slab avalanches. *Journal of Geophysical Research: Solid Earth*, 108(B2):2119.

Bebi, P., Kienast, F., and Schönenberger, W. (2001). Assessing structures in mountain forests as a basis for investigating the forests dynamics and protective function. *Forest Ecology and Management*, 145:3–14.

Brown, C. B., Evans, R. J., and LaChapelle, E. R. (1972). Slab avalanching and the state of stress in fallen snow. *Journal of Geophysical Research: Oceans and Atmospheres*, 77(24):4570–4580.

Faillettaz, J., Louchet, F., and Grasso, J. (2006). Cellular automaton modelling of slab avalanche triggering mechanisms: from the universal statistical behaviour to particular cases. In *Proceedings of the 2006 International Snow Science Workshop, Telluride, Colorado*, pages 174–180.

Feistl, T., Bebi, P., Teich, M., Bühler, Y., Christen, M., Thuro, K., and Bartelt, P. (2014). Observations and modeling of the braking effect of forests on small and medium avalanches. *Journal of Glaciology*, 60(219):124–138.

Gaume, J., Chambon, G., Eckert, N., and Naaim, M. (2012). Relative influence of mechanical and meteorological factors on avalanche release depth distributions: An application to French Alps. *Geophysical Research Letters*, 39:L12401.

Gubler, H. and Rychetnik, J. (1991). Effects of forests near the timberline on avalanche formation. In Bergmann, H., Lang, H., Frey, W., Issler, D., and Salm, B., editors, *Snow, Hydrology and Forests in High Alpine Areas Proceedings of the Vienna Symposium, August 1991.*, volume 205, pages 19–38. IAHS.

Hess, E. (1931). Wildschneelawinen. In *Die Alpen*, pages 321–334. SAC.

Ishikawa, M., Sato, S., and Kawaguchi, T. (1969). Stand density of avalanche prevention forest. *Journal of the Japanese Society of Snow and Ice*, 31(1):14–18.

Jamieson, B. and Johnston, C. D. (2001). Evaluation of the shear strength frame test for weak snowpack layers. *Annals of Glaciology*, 32(1):59–69.

Jamieson, B., Zeidler, A., and Brown, C. (2007). Explanation and limitations of study plot stability indices for forecasting dry snow slab avalanches in surrounding terrain. *Cold Regions Science and Technology*, 50:23–34.

Jamieson, J. B. and Johnston, C. D. (1990a). Insitu tensile tests of snow-pack layers. *Journal of Glaciology*, 36(122):102–106.

Jamieson, J. B. and Johnston, C. D. (1990b). The width of unconfined slab avalanches based on field measurements of slab

properties. In *International Snow Science Workshop, Bigfork, Montana USA, October 9-13,1990*.

Jamieson, J. B. and Johnston, C. D. (1992). A fracture-arrest model for unconfined dry slab avalanches. *Canadian Geotechnical Journal*, 29(1):61–66.

Lackinger, B. (1989). Supporting forces and stability of snow-slab avalanches: a parameter study. *Annals of Glaciology*, 13:140–145.

Ling, C.-H. (1985). A note on the density distribution of dry snow. *Journal of Glaciology*, 31:194–195.

Margreth, S. (2007). Defense structures in avalanche starting zones: Technical guideline as an aid to enforcement. Environment in Practice no. 0704, Federal Office for the Environment, Bern; WSL Swiss Federal Institute for Snow and Avalanche Research SLF, Davos, FOEN Documentation CH-3003 Bern.

McClung, D. and Schaerer, P. (2006). *The Avalanche Handbook*. The Mountaineers Books, 1011 SW Klickitat Way, Seattle, Washington 98134, 3rd edition.

McClung, D. M. (2003). Size scaling for dry snow slab release. *Journal of Geophysical Research*, 108(B10):2465.

McClung, D. M. (2009). Dimensions of dry snow slab avalanches from field measurements. *Journal of Geophysical Research: Earth Surface*, 114:F01006.

Meyer-Grass, M. and Schneebeli, M. (1992). Die Abhängigkeit der Waldlawinen von Standorts-, Bestandes- und Schneeverhältnissen. In *Internationales Symposion Interpraevent 1992-Bern*.

Olschewski, R., Bebi, P., Teich, M., Wissen Hayek, U., and Grét-Regamey, A. (2012). Avalanche protection by forests a choice experiment in the Swiss Alps. *Forest Policy and Economics*, 17:19–24.

Perla, R. (1977). Slab avalanche measurements. *Canadian Geotechnical Journal*, 14(2):206–213.

Perla, R., Beck, T. M. H., and Cheng, T. T. (1982). The shear strength index of alpine snow. *Cold Regions Science and Technology*, 6(1):11–20.

Rosenthal, W. and Elder, K. (2003). Evidence of chaos in slab avalanching. *Cold Regions Science and Technology*, 37:243–253.

Salm, B., Burkard, A., and Gubler, H. U. (1990). Berechnung von Fliesslawinen. Eine Anleitung für Praktiker mit Beispielen. Mitt. Eidgenöss. Inst. Schnee- Lawinenforsch. 47, Eidgenöss. Inst. Schnee- Lawinenforsch., SLF, Davos, Switzerland.

Saloranta, T. M. (2014). Simulating more accurate snow maps for Norway with MCMC parameter estimation method. *The Cryosphere Discusion*, 8:1973–2003.

Schläppy, R., Eckert, N., Jomelli, V., Stoffel, M., Grancher, D., Brunstein, D., Naaim, M., and Deschatres, M. (2014). Validation of extreme snow avalanches and related return periods derived from a statistical-dynamical model using tree-ring techniques. *Cold Regions Science and Technology*, 99:12–26.

Schweizer, J., Mitterer, C., and Stoffel, L. (2008). Determining the critical new snow depth for a destructive avalanche by considering the return period. In *Proceedings Whistler 2008 International Snow Science Workshop September 21-27, 2008*, pages 292–298.

Schweizer, J., Reuter, B., van Herwijnen, A., and Gaume, J. (2016). Avalanche release 101. In *Proceedings, International Snow Science Workshop, Breckenridge, Colorado, 2016*.

Sigrist, C. (2006). *Measurement of Fracture Mechanical Properties of Snow and Application to Dry Snow Slab Avalanche Release*. PhD thesis, Swiss Federal Institute of Technology Zurich.

Simenhois, R., Birkeland, K. W., and van Herwijnen, A. (2012). Measurements of ect scores and crack-face friction in non-persistent weak layers: What are the implications for practitioners? In *Proceedings, 2012 International Snow Science Workshop, Anchorage, Alaska*, pages 104–110.

Teich, M., Schneebeli, M., Bebi, P., Giunta, A. D., Gray, C. G., and Jenkins, M. J. (2016). Effects of bark beetle attacks on snowpack and snow avalanche hazard. In *Proceedings, International Snow Science Workshop, Breckenridge, Colorado, 2016*.

TEK17 (2017). Byggteknisk forskrift veiledning. Technical report, Direktoratet for byggkvalitet.

van Herwijnen, A. and Heierli, J. (2009). Measurement of crack-face friction in collapsed weak snow layers. *Geophysical Research Letters*, 36:L23502,.

Viglietti, D., Letey, S., Motta, R., Maggioni, M., and Freppaz, M. (2010). Snow avalanche release in forest ecosystems: A case study in the Aosta Valley Region (NW-Italy). *Cold Regions Science and Technology*, 64:167–173.

Zeidler, A. (2004). *Forecasting skier-triggered avalanches in the Columbia Mountains of Canada*. PhD thesis, University of Calgary.

Zeidler, A. and Jamieson, B. (2006). Refinements of empirical models to forecast the shear strength of persistent weak snow layers Part A: Layers of faceted crystals. *Cold Regions Science and Technology*, 44:194–205.